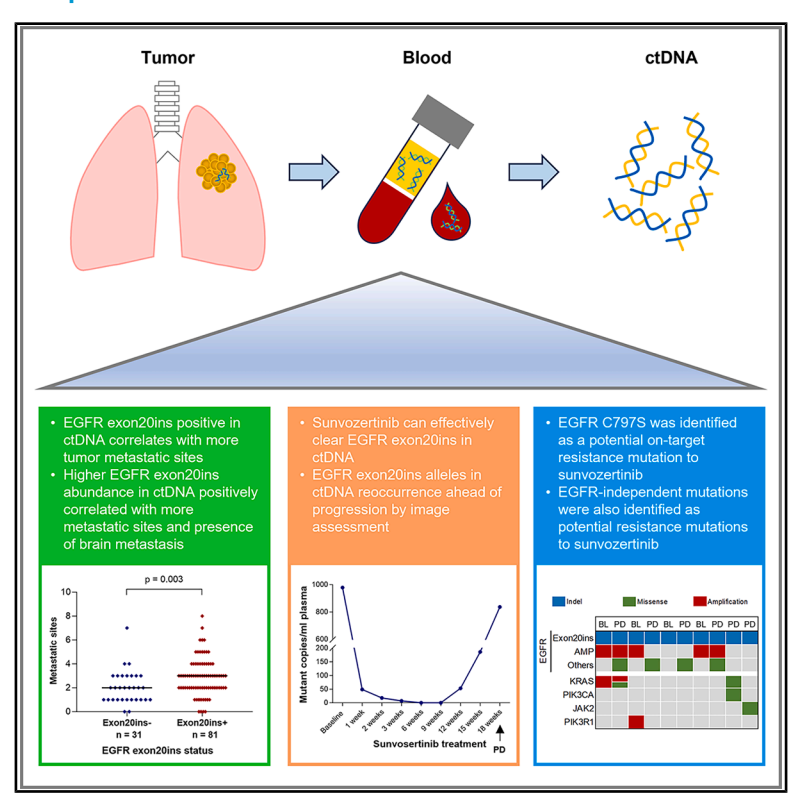


Genetic biomarker study of sunvozertinib for clinical prognosis and prediction in NSCLC with *EGFR* exon 20 insertion mutation

Graphical abstract



Authors

Yan Xu, James Chih-Hsin Yang, Yanqiu Zhao, ..., Li Zheng, Pasi A. Jänne, Mengzhao Wang

Correspondence

mengzhaowang@sina.com

In brief

Xu et al. show that *EGFR* exon20ins positivity and higher *EGFR* exon20ins abundance in ctDNA are correlated with advanced NSCLC. The earliest clearance of *EGFR* exon20ins in ctDNA occurs after 1 week of sunvozertinib treatment. Acquired *EGFR* C797S is a potential ontarget resistance mutation to sunvozertinib.

Highlights

- EGFR exon20ins positive in ctDNA is associated with advanced disease characteristics
- Sunvozertinib can effectively clear EGFR exon20ins in ctDNA
- Resistance to sunvozertinib can be through EGFRdependent and -independent mechanisms







Article

Genetic biomarker study of sunvozertinib for clinical prognosis and prediction in NSCLC with *EGFR* exon 20 insertion mutation

Yan Xu,^{1,49} James Chih-Hsin Yang,^{2,49} Yanqiu Zhao,³ Ludovic Doucet,⁴ Jianying Zhou,⁵ Yongsheng Wang,⁶ David Planchard,^{7,8} Yun Fan,⁹ Bo Jin,¹⁰ Zhigang Han,¹¹ Laurent Greillier,¹² Julien Mazieres,¹³ Meili Sun,¹⁴ Ying Hu,¹⁵ Xia Song,¹⁶ Cuimin Ding,¹⁷ Lin Wu,¹⁸ Kejing Tang,¹⁹ Li Liang,²⁰ Yu Yao,²¹ Ying Cheng,²² Yong He,²³ Bruna Pellini Ferreira,²⁴ François Ghiringhelli,²⁵ Enriqueta Felip,²⁶ Joaquim Bosch-Barrera,²⁷ Anwen Liu,²⁸

(Author list continued on next page)

(Affiliations continued on next page)

SUMMARY

This is a report of biomarker analysis for sunvozertinib, a leading epidermal growth factor receptor (EGFR) tyrosine kinase inhibitor (TKI) targeting *EGFR* exon 20 insertion mutation (exon20ins) non-small cell lung cancer (NSCLC). There is a positive correlation between positive *EGFR* exon20ins in plasma circulating tumor DNA (ctDNA) and advanced disease. Shorter progression-free survival and lower objective response rate (45.8% vs. 68.0%) were observed in patients with positive *EGFR* exon20ins compared to those with negative status. Droplet digital PCR analysis showed that the *EGFR* exon20ins allele in ctDNA decreased over time in 85.7% of patients, with the earliest clearance occurred after 1 week of sunvozertinib treatment. Acquired *EGFR* C797S is identified as a potential on-target resistance mutation to sunvozertinib. Finally, efforts are undertaken to investigate therapeutic approaches that aim to overcome the putative acquired resistance to sunvozertinib.

INTRODUCTION

Epidermal growth factor receptor (*EGFR*) exon 20 insertion mutations (exon20ins) account for around 2% of non-small cell lung cancer (NSCLC). More than 100 subtypes of *EGFR* exon20ins

have been reported, leading to disease heterogeneity and potential challenges for developing unified treatments.² In *EGFR*-mutant (*EGFR*m) NSCLC, an association between molecular factors and disease characteristics has been reported,³ while there are no reports available focused specifically on *EGFR* exon20ins



¹Peking Union Medical College Hospital, Chinese Academy of Medical Sciences & Peking Union Medical College, Beijing, China

²National Taiwan University Hospital and National Taiwan University Cancer Center, Taipei, Taiwan

³Affiliated Cancer Hospital of Zhengzhou University, Zhengzhou, China

⁴Institut de Cancérologie de l'Ouest (ICO) - René Gauducheau, Saint-Herblain, France

⁵The First Affiliated Hospital, Zhejiang University School of Medicine, Hangzhou, China

⁶West China Hospital, Sichuan University, Chengdu, China

⁷Gustave Roussy, Department of Medical Oncology, Thoracic Group, Villejuif, France

⁸Faculty of Medicine, Paris-Saclay University, Paris, France

⁹Zhejiang Cancer Hospital, Hangzhou, China

¹⁰The First Hospital of China Medical University, Shenyang, China

¹¹The Affiliated Cancer Hospital of Xinjiang Medical University, Urumgi, China

¹²CHU Hôpital de la Timone, Marseille, France

¹³CHU de Toulouse - Hôpital Larrey, Toulouse, France

¹⁴Central Hospital Affiliated to Shandong First Medical University, Jinan, China

¹⁵Beijing Chest Hospital, Capital Medical University, Beijing, China

¹⁶Shanxi Provincial Cancer Hospital, Taiyuan, China

¹⁷The Fourth Hospital of Hebei Medical University, Shijiazhuang, China

¹⁸Hunan Cancer Hospital, Changsha, China

¹⁹The First Affiliated Hospital, Sun Yat-sen University, Guangzhou, China

²⁰Peking University Third Hospital, Beijing, China

²¹The First Affiliated Hospital of Xi'an Jiaotong University, Xi'an, China

²²Jilin Cancer Hospital, Changchun, China



Yan Yu,²⁹ Xiaorong Dong,³⁰ Junzhen Gao,³¹ D. Ross Camidge,³² Weiqi Nian,³³ Chengzhi Zhou,³⁴ Runxiang Yang,³⁵ Thomas John,³⁶ Bo Gao,³⁷ Lyudmila Bazhenova,³⁸ Misako Nagasaka,³⁹ Jianghong Wang,⁴⁰ Xiubao Ren,⁴¹ Fei Xu,⁴² Wen Li,⁴³ Dahai Zhao,⁴⁴ Huijie Wang,⁴⁵ Si Sun,⁴⁵ Jian'an Huang,⁴⁶ Xuehua Zhu,⁴⁷ Li Zheng,⁴⁷ Pasi A. Jänne,⁴⁸ and Mengzhao Wang^{1,50,*}

²³Army Medical Center of PLA, Chongqing, China

²⁴H. Lee Moffitt Cancer Center & Research Institute, Tampa, FL, USA

²⁵Centre Georges François Leclerc, Dijon, France

²⁶Vall d'Hebron Institut d'Oncologia, Barcelona, Spain

²⁷Institut Catala d'Oncologia de Girona (ICO Girona), Girona, Spain

²⁸The Second Affiliated Hospital of Nanchang University, Nanchang, China

²⁹Harbin Medical University Cancer Hospital, Harbin, China

³⁰Union Hospital, Tongji Medical College, Huazhong University of Science and Technology, Wuhan, China

³¹The Affiliated Hospital of Inner Mongolia Medical University, Hohhot, China

32 University of Colorado Hospital, Anschutz Cancer Pavilion, Aurora, CO, USA

33Chongqing Cancer Hospital, Chongqing, China

³⁴The First Affiliated Hospital of Guangzhou Medical University, Guangzhou, China

35 Yunnan Cancer Hospital, Kunming, China

³⁶Peter MacCallum Cancer Centre, Melbourne, VIC, Australia

37Blacktown Hospital, Sydney, NSW, Australia

38University of California, San Diego (UCSD), Moores Cancer Center, La Jolla, CA, USA

39University of California Irvine Medical Center (UCIMC) - Chao Family Comprehensive Cancer Center, Orange, CA, USA

⁴⁰Chongqing University Cancer Hospital, Chongqing, China

⁴¹Tianjin Medical University Cancer Institute and Hospital, Tianjin, China

⁴²The First Affiliated Hospital of Nanchang University, Nanchang, China

⁴³The Second Affiliated Hospital, Zhejiang University School of Medicine, Hangzhou, China

⁴⁴The Second Hospital of Anhui Medical University, Hefei, China

⁴⁵Fudan University Shanghai Cancer Center, Shanghai, China

⁴⁶The First Affiliated Hospital of Soochow University, Suzhou, China

⁴⁷Dizal Pharmaceutical, Shanghai, China

⁴⁸Lowe Center for Thoracic Oncology, Dana-Farber Cancer Institute, Boston, MA, USA

⁴⁹These authors contributed equally

⁵⁰Lead contact

*Correspondence: mengzhaowang@sina.com https://doi.org/10.1016/j.xcrm.2025.102121

NSCLC. It is hypothesized that this type of biomarker analysis could help identify potential prognostic factors for this group of patients.

Currently, the golden standard for assessing gene mutations is to analyze tumor tissues. However, obtaining tumor samples through tissue biopsy, an invasive, costly, time-consuming, and potentially risky procedure, remains challenging in the clinic, especially for re-biopsy when the tumor progresses or relapses.4 In recent years, plasma circulating tumor DNA (ctDNA) emerges to be a promising alternative sample type for the detection of driver and resistance mutations, given its advantage of minimally invasive method for plasma sample collection. This approach enables obtaining genetic information when tissue biopsy is not possible and real-time monitoring of the clonal evolution.^{4,5} In addition, tumor heterogeneity is also problematic: a small biopsy sample may not be representative of the whole tumor. Patients with advanced cancer usually have multiple metastases, and thus how many tumor biopsy samples from different anatomic sites should be harvested to gain a holistic view of the disease remains to be determined. Since the blood bathes most tumor sites in patients with advanced cancers, it may be reasonable to speculate that plasma ctDNA might better reflect tumor heterogeneity than small tumor biopsies.6

Sunvozertinib (DZD9008) is an oral, potent, irreversible, and selective EGFR tyrosine kinase inhibitor (TKI) that has shown promising antitumor efficacy in patients with NSCLC with EGFR exon20ins. It has been granted breakthrough therapy designation by the US Food and Drug Administration (FDA) and China National Medical Products Administration. Through its phase 2 single-arm pivotal study (WU-KONG6; NCT05712902), sunvozertinib has been granted conditional approval in China for the treatment of NSCLC with EGFR exon20ins in the second-line or later-line setting. In addition, a multinational phase 1/2 study (WU-KONG1, NCT03974022) and a phase 3 study (WU-KONG28, NCT05668988) are ongoing to assess its antitumor efficacy globally. With sunvozertinib as an emerging effective treatment, it is of interest to investigate blood-based genetic biomarkers that could be associated with tumor response to sunvozertinib in NSCLC with EGFR exon20ins. In addition, it is also well known that acquired resistance inevitably occurs during EGFR TKI treatment, even in patients who exhibit an initial dramatic response. Therefore, it is also important to understand the resistance mechanism of sunvozertinib to help explore potential salvage strategies.

In this article, we report the results of blood-based genetic biomarker analysis in NSCLC with *EGFR* exon20ins, by pooling the data from three clinical studies, WU-KONG1 Part A

Article



Table 1. Demographic and base	eline characteristics		
Characteristics	Patient population ($n = 121$)		
Age			
Median age, years (range)	58 (32–82)		
Sex, n (%)			
Female	68 (56.2)		
Male	53 (43.8)		
Race, n (%)			
Asian	110 (90.9)		
White	11 (9.1)		
Smoking, n (%)			
Never	80 (66.1)		
Ever	41 (33.9)		
Baseline ECOG performance status			
0	36 (29.8)		
1	84 (69.4)		
Missing	1 (0.8)		
Histological type, <i>n</i> (%)			
Adenocarcinoma	114 (94.2)		
Adenosquamous carcinoma	2 (1.7)		
Squamous cell carcinoma	4 (3.3)		
Other	1 (0.8)		
Disease status at study entry, n (%)			
Locally advanced	6 (5.0)		
Metastatic	115 (95.0)		
Number of metastatic sites/lesions			
<3	62 (51.2)		
>3	59 (48.8)		
Brain metastasis, n (%)	()		
Yes	44 (36.4)		
No	77 (63.6)		
Prior lines of therapy, <i>n</i> (%)	11 (66.6)		
1	56 (46.3)		
>2	65 (53.7)		
Prior treatment, <i>n</i> (%)	00 (00.1)		
Chemotherapy	118 (97.5)		
Antiangiogenic therapy ^a	61 (50.4)		
EGFR TKI ^b	41 (33.9)		
Anti-PD-1/PD-L1 therapy	41 (33.9)		
Amivantamab	5 (4.1)		
Other	. ,		
	20 (16.5)		
Dose, n (%)	9 (6 6)		
200 mg	8 (6.6)		
300 mg 400 mg	106 (87.6)		
	7 (5.8)		
EGFR exon20ins status in plasma o			
Positive	81 (66.9)		
V769_D770insASV	34 (42.0)		
D770_N771insSVD	12 (14.8)		
Others	35 (43.2)		

Table 1. Continued	
Characteristics	Patient population ($n = 121$)
Negative	31 (25.6)
Unknown	9 (7.4)

ctDNA, circulating tumor DNA; ECOG, Eastern Cooperative Oncology Group; EGFR, epidermal growth factor receptor; exon20ins, exon 20 insertion mutation; TKI, tyrosine kinase inhibitor.

^aAntiangiogenic therapies included anti-VEGF and anti-VEGFR anti-bodies.

^bEGFR TKIs included afatinib, almonertinib, erlotinib, furmonertinib, gefitinib, icotinib, lazertinib, mobocertinib, osimertinib, and poziotinib.

(WU-KONG1A), WU-KONG2 (Chinadrugtrial: CTR20192097), and WU-KONG6. From these three studies, patients with NSCLC harboring *EGFR* exon20ins with different demographics and disease characteristics, who had received at least one prior line of systemic anticancer therapy and received sunvozertinib treatment at different dose levels, were included in the analysis. Plasma ctDNA was used for the genetic profiling of *EGFR* and its downstream signaling pathways. In addition, the association between genetic biomarkers and tumor responses was also analyzed. Furthermore, acquired mutations in patients who relapsed after sunvozertinib treatment were explored.

RESULTS

The original cohort Patient characteristics

A total of 121 patients with NSCLC with *EGFR* exon20ins were included in this genetic biomarker analysis. Patient demographics and disease characteristics are summarized in Table 1. The majority of patients (94.2%) had adenocarcinoma. Around 70% of patients had baseline Eastern Cooperative Oncology Group performance score of 1. The majority of patients (95.0%) had metastatic NSCLC, and 36.4% had brain metastasis. More than half (53.7%) had received at least two prior lines of therapies. All patients received sunvozertinib monotherapy at doses ranging from 200 to 400 mg once daily (QD), with the majority (87.6%) having received the dose/regimen of 300 mg QD. All patients included in the analysis had baseline plasma samples collected (Figure S1).

Correlation between EGFR exon20ins and clinical characteristics

Among the 121 patients, 81 (66.9%) were confirmed to harbor *EGFR* exon20ins in plasma ctDNA by retrospective central testing using next-generation sequencing (NGS), and 31 (25.6%) were *EGFR* exon20ins negative. The *EGFR* exon20ins status in plasma ctDNA of nine patients was unknown due to low DNA quantity or not achieving sufficient unique sequencing depths as required by NGS (Figure S1; Tables 1 and S1). There were 25 *EGFR* exon20ins subtypes identified by retrospective central testing. *EGFR* V769_D770insASV (ASV) and D770_N771insSVD (SVD) were the most common *EGFR* exon20ins subtypes, accounting for 42% and 14.8% of *EGFR* exon20ins-positive samples, respectively (Table 1; Figure S2).



Table 2. Correlation between *EGFR* exon20ins status in baseline plasma ctDNA and clinical characteristics

		Plasma EGF	R exon20ins	status
Characteristics	n	Positive	Negative	p value
Age in years				
<60, n (%)	62	46 (74.2%)	16 (25.8%)	0.674
≥60, <i>n</i> (%)	50	35 (70.0%)	15 (30.0%)	_
Sex				
Female, n (%)	60	46 (76.7%)	14 (23.3%)	0.296
Male, n (%)	52	35 (67.3%)	17 (32.7%)	_
Race				
Asian, <i>n</i> (%)	106	77 (72.6%)	29 (27.4%)	0.668
Non-Asian, n (%)	6	4 (66.7%)	2 (33.3%)	_
Smoking				
Ever, n (%)	40	26 (65.0%)	14 (35.0%)	0.270
Never, n (%)	72	55 (76.4%)	17 (23.6%)	_
Disease status at study ent	ry			
Locally advanced, n (%)	6	4 (66.7%)	2 (33.3%)	0.668
Metastatic, n (%)	106	77 (72.6%)	29 (27.4%)	-
Number of metastatic sites	/lesio	ns at study e	ntry	
<3, n (%)	56	35 (62.5%)	21 (37.5%)	0.034
≥3, <i>n</i> (%)	56	46 (82.1%)	10 (17.9%)	-
Brain metastasis				
Yes, n (%)	41	34 (82.9%)	7 (17.1%)	0.079
No, n (%)	71	47 (66.2%)	24 (33.8%)	_
Prior lines of therapy ^a				
1, n (%)	51	37 (72.5%)	14 (27.5%)	>0.999
≥2, <i>n</i> (%)	61	44 (72.1%)	17 (27.9%)	_

The Fisher's exact test was applied for the analysis. Significance was established when the p value was less than 0.05. All tests were two-sided. ctDNA, circulating tumor DNA; EGFR, epidermal growth factor receptor; exon20ins, exon 20 insertion mutation; TKI, tyrosine kinase inhibitor. aPrior therapies included chemotherapy, antiangiogenic therapy, EGFR TKI, anti-PD-1/PD-L1 therapy, amivantamab, and others.

We then evaluated the correlation between *EGFR* exon20ins status in baseline plasma ctDNA and demographics/baseline disease characteristics. Compared to patients with negative *EGFR* exon20ins, patients with positive *EGFR* exon20ins had more metastatic sites/lesions (p = 0.034 in Table 2; p = 0.003 in Figure 1A) and greater tumor volume (p = 0.004 in Figure 1B). In contrast, no correlation of *EGFR* exon20ins status with other characteristics, such as age, sex, race, history of smoking, disease status, or number of prior lines of therapy, was observed, while there was a trend showing correlation with baseline brain metastasis (Table 2).

Further analysis in positive *EGFR* exon20ins population showed that higher abundance of *EGFR* exon20ins in ctDNA was detected in patients with more metastatic sites/lesions (p = 0.003) and brain metastasis (p = 0.024) (Figures 1C and 1D), while no correlation was observed with other characteristics (Figure S3).

Correlation between EGFR exon20ins and antitumor efficacy of sunvozertinib

As 300 mg was determined as the recommended phase 2 dose as well as the dose for marketing, we analyzed the correlation

between *EGFR* exon20ins status and its abundance in plasma ctDNA, with clinical endpoints (objective response rate [ORR] and progression-free survival [PFS]) at this dose level. The ORR and median PFS of the patients treated with sunvozertinib were 50% (53/106) and 5.6 months, respectively. When comparing the ORRs between patients with positive (n = 72) or negative (n = 25) *EGFR* exon20ins in ctDNA, we observed a higher ORR in the negative group, compared to that of the positive group (68% vs. 45.8%), though no statistical significance was reached (Figure 1E). In addition, there was longer median PFS in the negative group, compared to that of the positive group, with statistical significance (negative vs. positive: 7.4 months vs. 5.5 months, p = 0.022) (Figure 1F).

We then conducted a further analysis in the patient population with positive EGFR exon20ins and observed a trend showing worse clinical response in patients with higher abundance of EGFR exon20ins (Figure 1G). Further, we divided the positive group into two subgroups: low abundance and high abundance of EGFR exon20ins, using 3.7% (median value) as a cutoff value, but did not observe a significant difference of ORR (50% vs. 41.7%, p = 0.637) (Figure 1H) or median PFS (5.6 months vs. 4.5 months, p = 0.191) (Figure 1I). Moreover, we also performed biomarker analysis in patients with baseline brain metastasis. Among all patients treated with sunvozertinib at 300 mg, 37.7% (40/106) had baseline brain metastasis. The ORR and median PFS of these patients were 40% (16/40) and 4.4 months, respectively. A numerically higher ORR was observed in patients with negative EGFR exon20ins compared to those with positive status at baseline (57.1% vs. 33.3%, p = 0.39) (Figure S4A), while no difference on median PFS (negative vs. positive: 4.1 months vs. 4.1 months, p = 0.359) was observed (Figure S4B).

Dynamic changes of ctDNA EGFR exon20ins quantity predicted antitumor activity of sunvozertinib

A total of 34 patients had available longitude plasma samples collected for the dynamic assessment of EGFR exon20ins copy number by droplet digital PCR (ddPCR). A high concordance of EGFR exon20ins positivity/negativity in baseline plasma ctDNA tested by NGS and ddPCR was observed (Figure 2A). In 14 patients with detectable EGFR exon20ins in baseline plasma ctDNA (4-4,051 EGFR exon20ins copies/mL plasma) who received sunvozertinib treatment at 300 mg, EGFR exon20ins mutant alleles decreased over time in 12 (85.7%) patients, and EGFR exon20ins was cleared in 11 (78.6%) patients during the first 6 weeks of treatment. The earliest clearance occurred after 1 week of sunvozertinib treatment (Figure 2B). There was a trend showing that there was a correlation with clinical benefit in those with a decrease or clearance of EGFR exon20ins. In five patients who had available longitudinal samples collected from baseline until disease progression with detectable EGFR exon20ins in ctDNA at baseline, EGFR exon20ins clearance during treatment, and EGFR exon20ins recurrence, EGFR exon20ins reoccurred at a median of 15 weeks (range: 3-21 weeks), ahead of disease progression by image assessments (Figure S5). In 17 patients with undetectable EGFR exon20ins in baseline plasma ctDNA treated with 200, 300, or 400 mg of sunvozertinib, the majority of patients (16/17) maintained undetectable levels in their follow-up longitudinal plasma samples.

Article



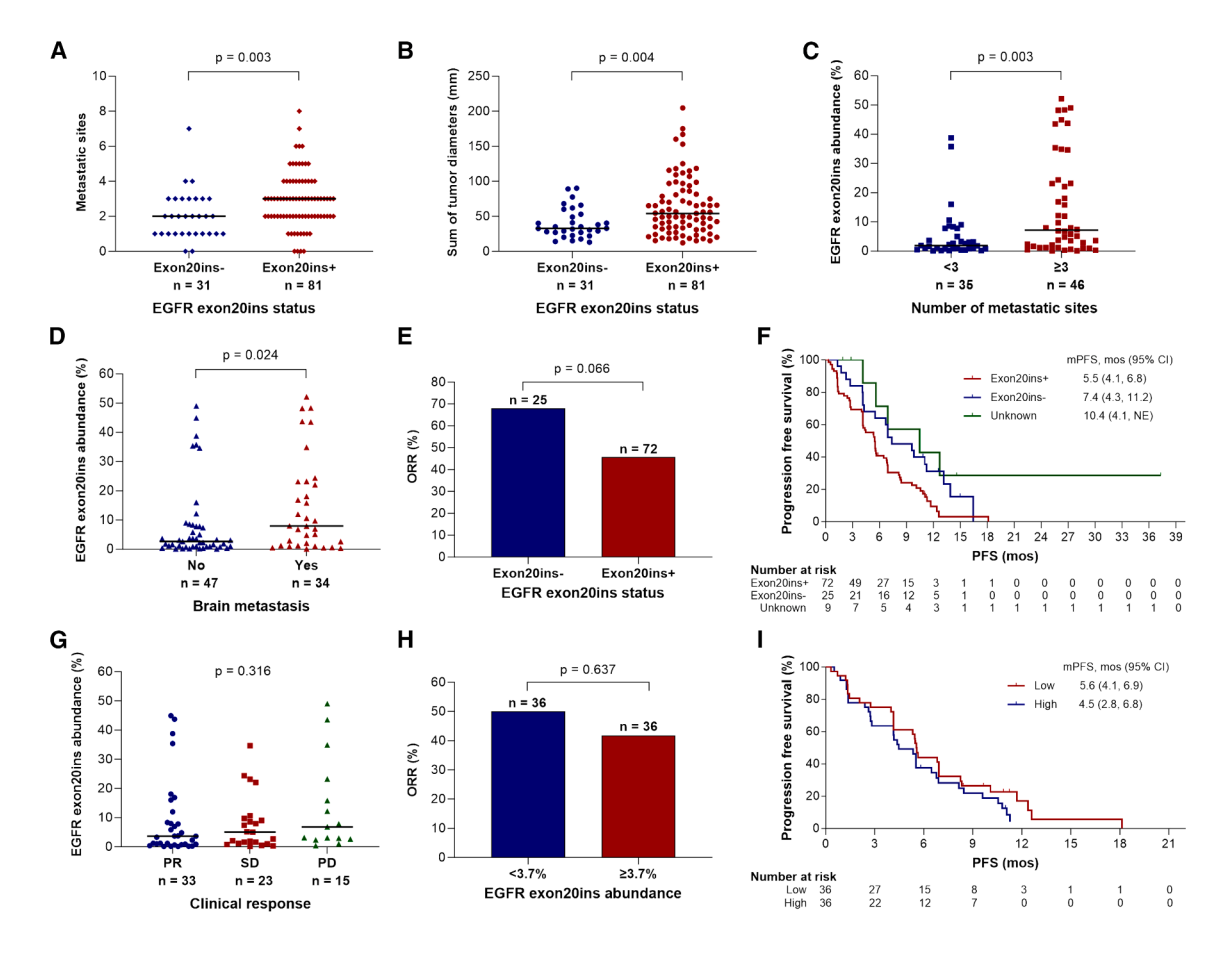


Figure 1. Correlations between EGFR exon20ins in baseline plasma ctDNA and the number of metastatic sites, brain metastasis, and tumor response with sunvozertinib

- (A) Metastatic sites/lesions of patients with negative or positive EGFR exon20ins in ctDNA.
- (B) Sum of tumor diameters of patients with negative or positive EGFR exon20ins in ctDNA.
- (C) EGFR exon20ins abundance in patients with low number (<3) versus high number (≥3) of metastatic sites/lesions.
- (D) EGFR exon20ins abundance in patients with or without baseline brain metastasis.
- (E) ORRs in patients with negative or positive EGFR exon20ins in ctDNA.
- (F) Kaplan-Meier analysis of PFS according to EGFR exon20ins status in ctDNA. EGFR exon20ins status (positive or negative) was defined by NGS. EGFR exon20ins status was unknown due to too low DNA quantity or not achieving sufficient unique sequencing depths as required by NGS.
- (G) EGFR exon20ins abundance in patients with different tumor responses. One patient non-evaluable for tumor response was not included in the analysis.
- (H) ORRs in patients with low or high abundance of EGFR exon20ins in ctDNA.
- (I) Kaplan-Meier analysis of PFS according to $\it EGFR$ exon 20 ins abundance in ctDNA.

The Mann-Whitney test was used for the analysis in (A), (B), (C), (D), and (G). Fisher's exact test was used for the analysis in (E) and (H). Significance was established when the p value was less than 0.05. All tests were two-sided. No further pairwise comparison was performed in (G) given the overall test was not significant. The heavy lines in (A) and (B) represent the median numbers of metastatic sites/lesions and median sums of the longest diameters of the target lesions in each group, respectively. The heavy lines in (C), (D), and (G) represent the median values of EGFR exon20ins abundance in each group. In (E)–(I), efficacy data at 300 mg were used for the analysis. In (F) and (I), median PFS was estimated by Kaplan-Meier method with 95% CIs. In (H) and (I), the median value of EGFR exon20ins abundance ((3.7%)) was used as a cutoff value to divide patients into two groups: low abundance ((3.7%)) and high abundance ((3.7%)). CI, confidence interval; ctDNA, circulation tumor DNA; EGFR, epidermal growth factor receptor; exon20ins, exon 20 insertion mutation; mos, months; mPFS, median progression-free survival; NE, not evaluable; NGS, next-generation sequencing; ORR, objective response rate; PD, progressive disease; PFS, progression-free survival; PR, partial response; SD, stable disease.

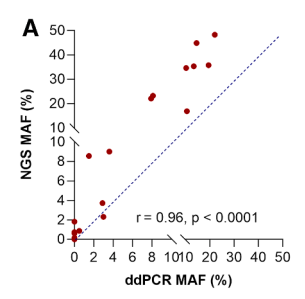
Potential resistance mechanisms to sunvozertinib

Eighteen patients who initially responded to sunvozertinib treatment but later developed disease progression met the criteria for acquired resistance⁹ and had available plasma ctDNA samples collected and were included in this analysis for genetic resistance mechanisms (Figure S1). NGS was used to identify poten-

tial genetic aberrations in *EGFR* and its downstream signaling pathways, which might be related to resistance to sunvozertinib.

Among the 18 patients, 12 had detectable *EGFR* exon20ins in ctDNA at disease progression, while three were *EGFR* exon20ins negative. Three patients were ctDNA *EGFR* exon20ins negative at both baseline and disease progression. Among the 12 patients





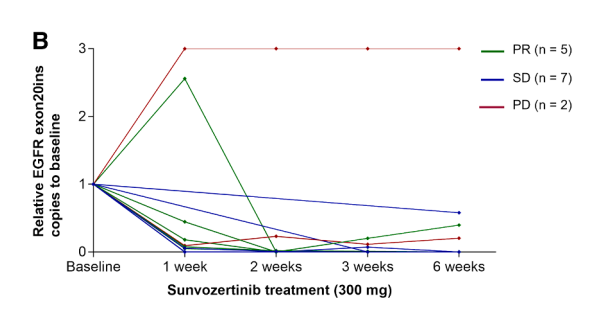


Figure 2. Dynamic changes of *EGFR* exon20ins DNA copy number in plasma ctDNA with sunvozertinib treatment

(A) Correlation between mutant allele frequency (MAF) of EGFR exon20ins in baseline plasma ctDNA samples tested by next-generation sequencing (NGS) and droplet digital PCR (ddPCR). Among the 34 patients with available MAF of EGFR exon20ins tested by ddPCR, seven patients did not have MAF of EGFR exon20ins tested by NGS due to too low DNA quantity or not achieving sufficient unique sequencing depths as required by NGS. Thus, MAF of EGFR exon20ins

in baseline plasma ctDNA of 27 patients tested by NGS and ddPCR was used for the analysis. Each dot represents the MAF of EGFR exon20ins tested by NGS and ddPCR. Pearson's correlation coefficient was applied for the analysis.

(B) Dynamic changes of *EGFR* exon20ins DNA copy number with sunvozertinib treatment at 300 mg, and association with tumor response. ddPCR, droplet digital PCR; EGFR, epidermal growth factor receptor; exon20ins, exon 20 insertion mutation; MAF, mutant allele frequency; NGS, next-generation sequencing; PD, progressive disease; PR, partial response; SD, stable disease.

with detectable EGFR exon20ins at disease progression, different mutation patterns at disease progression were observed. In addition to EGFR exon20ins, two patients had EGFR C797S mutations, one had EGFR C797S and KRAS mutation, one had EGFR G724S, one had KRAS mutation and PIK3CA mutation, and one had JAK2 mutation (Figure 3A; Table S2). Interestingly, all the acquired EGFR C797S were in cis with EGFR exon20ins (Figures 3B-3D), similar to that found in osimertinib resistance, where C797S was in cis with EGFR T790M mutation. 10 We further analyzed the time course of C797S development and performed ddPCR in serial plasma samples from the three patients with detectable C797S (Figures 3E-3G). At baseline, the three patients had detectable ctDNA EGFR exon20ins with 77-2.740 copies/mL plasma, while none of the three patients had de novo EGFR C797S. For subject 001, EGFR exon20ins in ctDNA increased 6 weeks earlier than EGFR C797S appearance and also earlier than disease progression confirmed by image scans. In addition, at disease progression, the ctDNA abundance of EGFR C797S was lower than that of EGFR exon20ins, consistent with the findings from NGS (Figure 3E). For subject 007, at the last time point of sample collection, neither EGFR exon20ins nor EGFR C797S was detected by ddPCR due to ctDNA quantity below the detection limit, though EGFR exon20ins copy numbers were detectable at 5 weeks and 20 weeks of sunvozertinib treatment (Figure 3F). For subject 023, EGFR exon20ins and C797S increased at the same time point, which was 3 weeks earlier than disease progression confirmed by image scans, and the ctDNA abundance of EGFR C797S was lower than EGFR exon20ins, consistent with the findings by NGS (Figure 3G).

The observation of secondary *EGFR* C797S at the time of disease progression in relapsed patients was not surprising. *EGFR* C797S was not only well known to confer resistance to osimertinib by preventing its binding to the EGFR active site, ¹¹ but it was also reported to confer resistance to mobocertinib, the TKI targeting *EGFR* exon20ins. ¹² Based on our previously reported 3D docking model of sunvozertinib and *EGFR* exon20ins, ¹³ C797S is located in the vicinity of the ATP-binding pocket, suggesting that a point mutation at this residue may disturb the binding of sunvozertinib with *EGFR* exon20ins. To validate this hypothesis, we generated Ba/F3

cells stably expressing EGFR exon20ins SVD mutant protein without or with C797S (SVD-C797S) and investigated the anti-proliferation activity of sunvozertinib. We found that cells expressing SVD-C797S double-mutant protein were markedly less sensitive to sunvozertinib, compared with cells only expressing EGFR exon20ins SVD mutant protein (Figure 3H). Consistently, sunvozertinib did not significantly inhibit pEGFR, even at a concentration of 3 μ M, in cells expressing EGFR SVD-C797S double-mutant protein (Figure 3I). These data suggested that *EGFR* C797S could be a mediator of acquired resistance to sunvozertinib. This finding was further confirmed in another cell model, which was engineered by stably expressing EGFR SVD-C797S mutant protein in lung cancer cell line KLN205 (Figure 3J).

The independent validation cohort

To further validate the correlation between *EGFR* exon20ins status in baseline plasma ctDNA and clinical characteristics and clinical endpoints, an independent validation cohort of 63 patients from a multinational phase 2 pivotal clinical study WU-KONG1 Part B (WU-KONG1B)¹⁴ was included (Figure S6). In this cohort, the majority of patients (81%) were non-Asian. By adding this independent cohort, the biomarker analysis could potentially address the question about the diversity of races. Other characteristics of the patients were comparable to the original cohort (Table S3).

Correlation between EGFR exon20ins and clinical characteristics

Among the 63 patients, 48 (76.2%) were confirmed to harbor *EGFR* exon20ins in plasma ctDNA by retrospective central testing using NGS, and 15 (23.8%) were *EGFR* exon20ins negative (Tables S3 and S4). The correlation between *EGFR* exon20ins status and demographics/disease characteristics in general aligned with that of the original cohort. Patients with positive *EGFR* exon20ins also had more metastatic sites/lesions (p < 0.001 in Table S5; p < 0.001 in Figure S7A), consistent with those of the original cohort. There was also a trend that higher *EGFR* exon20ins abundance correlated with greater tumor volume, though no statistical significance was detected (p = 0.637 in Figure S7B), which might be due to the relatively small sample size. No correlation of *EGFR* exon20ins status





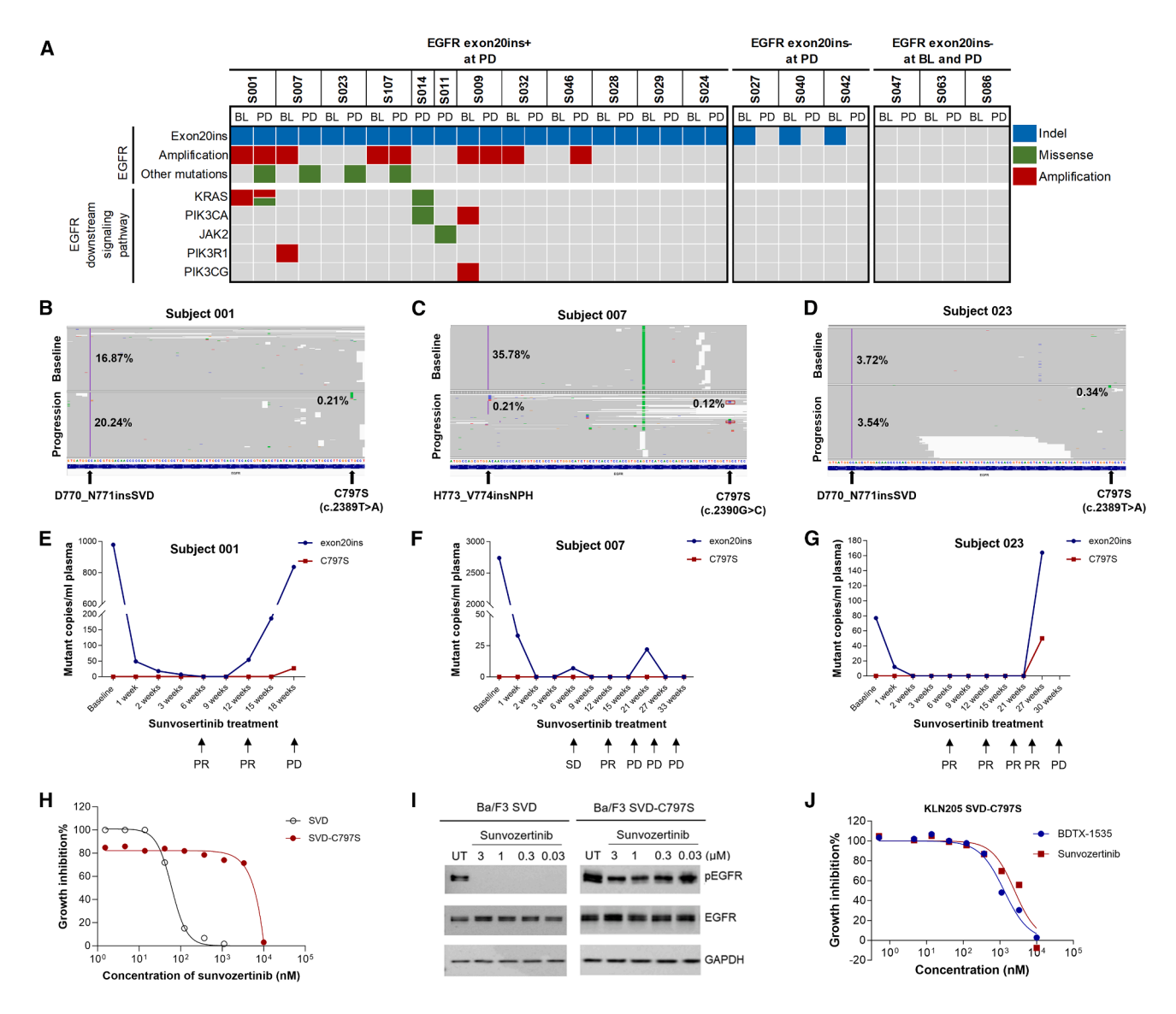


Figure 3. Potential genetic resistance mechanism of sunvozertinib

(A) Genetic characteristics potentially related to resistance to sunvozertinib by next-generation sequencing.

(B–D) In the index cases (subjects #001, 007, and 023), EGFR C797S mutation was identified at disease progression or time point around disease progression confirmed by image scans. Overlapping reads spanning EGFR exon20ins location and C797 contained both exon20ins and C797S mutations, indicating that the two mutations occurred in cis on the same allele.

(E-G) Longitudinal monitoring of EGFR exon20ins and C797S mutation during the treatment by using droplet digital PCR.

- (H) Anti-proliferative effect of sunvozertinib in Ba/F3 cells expressing EGFR exon20ins SVD or SVD-C797S double-mutant protein.
- (I) Inhibition of pEGFR pathway with sunvozertinib in Ba/F3 cells expressing EGFR exon20ins SVD-C797S double-mutant protein.

(J) Anti-proliferation activity of sunvozertinib or BDTX-1535 on KLN205 cells engineered with *EGFR* exon20ins SVD-C797S double mutations. BL, baseline; EGFR, epidermal growth factor receptor; exon20ins, exon 20 insertion mutation; PD, progressive disease; PR, partial response; SD, stable disease; SVD, D770_N771insSVD.

with other characteristics, such as age, sex, race, history of smoking, disease status, baseline brain metastasis, or number of prior lines of therapy, was observed either (Table S5). There was also a trend of higher abundance of *EGFR* exon20ins in patients with more metastatic sites/lesions (Figure S7C). A higher abundance of *EGFR* exon20ins in ctDNA was also etected in patients with baseline brain metastasis (p = 0.038) (Figure S7D). No correlation between abundance of *EGFR* exo-

n20ins and other characteristics was observed except race, which might be due to the small sample size of Asian patients (Figure S8).

Correlation between EGFR exon20ins and antitumor efficacy of sunvozertinib

The ORR and median PFS of the patients treated with sunvozertinib at 300 mg in the independent cohort were 51.2% and 6.9 months, with a median follow-up of 12.3 months,



respectively. The trend of correlation between *EGFR* exon20ins status at baseline and clinical endpoints aligned with that of the original cohort (Figures S7E–S7I). Among the patients treated with sunvozertinib at 300 mg, 29.3% (12/41) of patients had baseline brain metastasis. The ORR and median PFS of these patients were 58.3% (7/12) and 4.4 months, respectively. In patients with positive *EGFR* exon20ins, the ORR and median PFS were 60% (6/10) and 5.5 months, respectively. There were two patients with negative *EGFR* exon20ins, and among them, one achieved partial response and PFS of 17.8 months, and another one had stable disease with PFS of 4.3 months.

Dynamic changes of ctDNA EGFR exon20ins quantity predicted antitumor activity of sunvozertinib

There were 39 patients who received sunvozertinib treatment at 300 mg and had available ddPCR data. Among them, 19 patients had detectable EGFR exon20ins at baseline (9-13,917 EGFR exon20ins copies/mL plasma). Decrease of EGFR exon20ins alleles over time was observed in 17 (89.5%) patients, and clearance of EGFR exon20ins was observed in 15 (78.9%) patients during the first 6 weeks of treatment. The earliest clearance occurred after 1 week of sunvozertinib treatment (Figure S9). In eight patients who had available longitudinal samples collected from baseline until disease progression with detectable EGFR exon20ins at baseline, EGFR exon20ins clearance during treatment, and EGFR exon20ins recurrence, EGFR exon20ins reoccurred with a median time of 7 weeks (range: 0-21 weeks), ahead of disease progression by image assessments (Figure S10). In 16 patients with undetectable EGFR exon20ins at baseline and who were treated with sunvozertinib at 300 mg, EGFR exon20ins remained undetectable during follow-up longitudinal plasma samples in the majority of patients (14/16, 87.5%). These findings were consistent with those of the original cohort.

Potential resistance mechanisms to sunvozertinib

Eight patients in the validation cohort met the criteria of acquired resistance and had available plasma ctDNA samples collected at disease progression (Figure S6). Successful sequencing data for exploration of resistance mechanism were obtained from seven patients, and among them, four had detectable *EGFR* exon20ins at disease progression, and three were *EGFR* exon20ins negative at both baseline and disease progression. No *EGFR* C797S was detected. Only one patient had *BRAF* amplification (Figure S11; Table S6).

Potential approaches to overcome resistance

Then, we explored potential treatment approaches to overcome resistance to sunvozertinib. Firstly, we investigated whether the fourth-generation EGFR TKIs targeting C797S could overcome such resistance or not. In this case, the most advanced fourth-generation EGFR TKI, BDTX-1535, ¹⁵ was studied in the cell model carrying the *EGFR* SVD-C797S double mutations. The results showed that BDTX-1535 failed to potently inhibit cell growth (Figure 3J), probably due to lack of activity against *EGFR* exon20ins. Then, we hypothesized that a chemotherapy-based combination strategy might be a more effective approach given that activation of more than one pathway was observed in patients who developed resistance to sunvozertinib treatment in later-line settings (as shown in Figure 3A). It has been reported that the activated compensatory signaling

pathway of interleukin-6/JAK/signal transducer and activator of transcription 3 (STAT3) with EGFR TKI treatment might contribute to resistance. ¹⁶ In addition to direct effects on tumor cells, targeting the JAK/STAT axis has also been proposed as a potential effective approach to reduce tumor-promoting immunosuppressive myeloid-derived suppressor cells, thereby counteracting malignant progression. ¹⁷ To test this hypothesis, we evaluated a JAK inhibitor golidocitinib, which blocks the JAK/STAT pathway, ¹⁸ in combination with platinum-based chemotherapy to overcome resistance of sunvozertinib. As shown in Figures 4A and 4B, combination of golidocitinib with chemotherapy showed encouraging antitumor activity in a xenograft model established with the *EGFR* exon20ins SVD-C797S double-mutant cells. As a control, there was no difference on EGFR expression (Figure 4C).

DISCUSSION

This is a report to analyze the characteristics of genetic biomarkers in EGFR exon20ins NSCLC in a large sample size of more than 100 patients and the correlation of the findings with outcomes in patients treated with an EGFR exon20ins-selective TKI sunvozertinib. It has been reported that in EGFRm NSCLC, plasma ctDNA is a widely used sample type for exploring correlations between genetic biomarkers and disease characteristics as well as clinical efficacy, given its convenience of sample collection and feasibility of longitudinal monitoring of changes, compared with that of tumor tissue. 19 In this article, we analyzed the correlation between EGFR exon20ins status in plasma ctDNA and clinical characteristics in more than 100 patients and validated the findings in an independent cohort. Patients with advanced-stage NSCLC with EGFR exon20ins who had received at least one prior line of systemic anticancer therapy were included, whose characteristics were also consistent with the advanced-stage disease characteristics. More than 50% had received >2 prior lines of therapies. This was in line with the current clinical practice of EGFR exon20ins NSCLC. Although the combination of amivantamab, a bispecific antibody, with carboplatin and pemetrexed was recently approved as a standard treatment by the US FDA,20 chemotherapy was still the most commonly used treatment in the first-line setting. In addition, the EGFR TKI mobocertinib was granted accelerated approval based on a single-arm extension cohort (EXCLAIM) of a phase 1/2 study²¹ but failed to improve PFS compared to platinum-based chemotherapy in its confirmatory phase 3 EXCLAIM-2 study and was thus withdrawn from the market.²² In this advanced-stage patient population, EGFR exon20ins ctDNA was detectable in 66.9%-76.2% of baseline plasma ctDNA specimens, comparable to the EGFR mutation detection rates in EGFRm NSCLC.23,24

We then investigated the correlation between plasma ctDNA *EGFR* exon20ins status and disease characteristics and found that *EGFR* exon20ins positivity was correlated with a greater number of metastatic sites/lesions and greater tumor volume. In addition, there was also a trend showing that patients with baseline brain metastasis had higher *EGFR* exon20ins ctDNA detection rates, in line with published results of *EGFR*m NSCLC.²⁵ The amount of ctDNA shedding into the blood has

Article



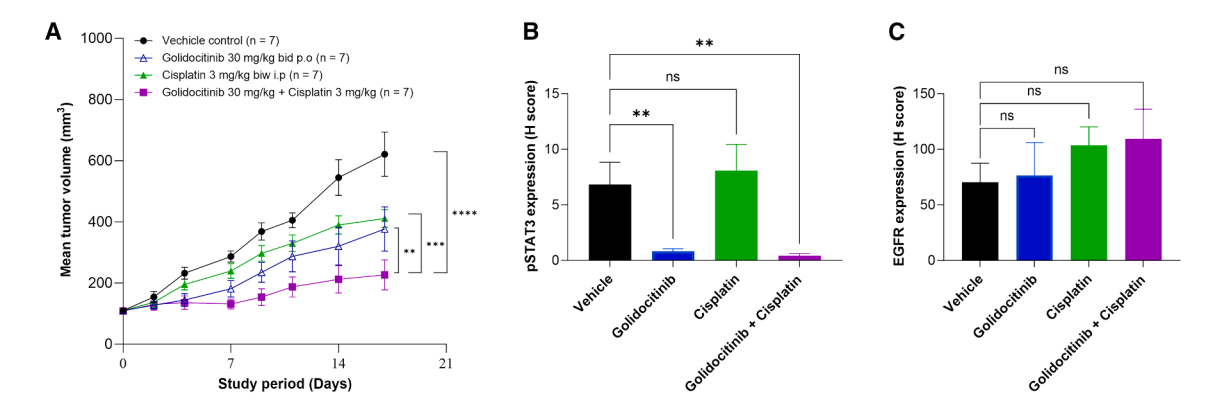


Figure 4. Antitumor activity of a JAK inhibitor golidocitinib in combination with chemotherapy in a xenograft model expressing EGFR exon20ins SVD-C797S

(A) Tumor growth inhibition of a xenograft model expressing EGFR with exon 20 ins SVD and C797S by different treatments. Error bars represent the standard error of mean of the individual means. Two-way ANOVA analysis was used to compare treatment groups to vehicle control group. **p < 0.01; ***p < 0.0005; ****p < 0.0001.

(B) pSTAT3 signals and (C) EGFR expression in tumor tissues post treatment. The tumor tissues from each treatment were collected at 2 h post the last dose of treatment (three mice per group). Error bars represent the standard deviation of individual means. Statistical analysis was performed using one-way ANOVA with Dunnett test. **p < 0.01; ns, not significant. Bid, twice daily; biw, twice weekly; EGFR, epidermal growth factor receptor; exon20ins, exon 20 insertion mutation; STAT3, signal transducer and activator of transcription 3; SVD, D770_N771insSVD; i.p., intraperitoneally; p.o., orally.

been reported to be affected by many factors, such as tumor location, size, metastasis, vascular infiltration, tumor status, and stage, and the amount of ctDNA released from tumor cells increased with the progression of metastasis. 19 Our findings were in line with these previous findings. In addition, our study also found that patients with more metastatic sites/lesions and brain metastasis had significantly higher ctDNA abundance of EGFR exon20ins, which further demonstrated that the amount of ctDNA shedding into the blood reflected tumor burden.²⁶ Baseline plasma EGFRm was reported to be prognostic and predictive of clinical benefit with osimertinib, and plasma EGFRm clearance at week 3 was reported to be correlated with improved PFS with osimertinib or osimertinib with the addition of platinum-pemetrexed chemotherapy.^{27,28} In this study, we also found better PFS and a trend of higher ORR in patients with negative EGFR exon20ins status, compared with those with positive status, which in part could be due to lower tumor burden in these patients. Overall, the findings in the independent validation cohort aligned with those of the original cohort.

In general, the change of *EGFR* exon20ins mutant alleles is related to the course of disease and also reflects tumor response to treatment. Therefore, continuously monitoring *EGFR* mutation during the course of disease could help better manage patients with NSCLC, e.g., for early identification of disease progression. Plasma ctDNA longitudinal monitoring was also reported to be useful to assess mutation status and disease progression in patients with NSCLC treated with mobocertinib.²⁹ In addition, the prognostic value of assessing *EGFR* exon20ins mutant alleles in ctDNA has been demonstrated.^{30,31} In this analysis, we observed a decrease or even clearance of ctDNA *EGFR* exon20ins mutant allele over time during sunvozertinib treatment, providing direct evidence of sunvozertinib targeting the *EGFR* exon20ins pathway, and *EGFR* exon20ins reoccurrence in ctDNA at a median of

7-15 weeks ahead of disease progression by image assessments, suggesting its predictive potential for disease progression.

Despite initial tumor response to sunvozertinib treatment, a certain proportion of patients eventually developed disease progression over time. Therefore, it is important to characterize the mechanism of resistance at the time of disease progression. This would help to shed light on potential subsequent therapies. In this analysis, we found diversified characteristics of genetic aberrations in patients who relapsed from sunvozertinib treatment, e.g., acquired EGFR C797S and other genetic resistance mutations. Acquired EGFR T790M was not observed in our analysis with a sample size of 18 and an additional independent cohort of seven patients. This is different from the reported data on poziotinib and mobocertinib. Acquired secondary EGFR T790M was observed in preclinical poziotinibresistant models and confirmed in patients who developed resistance to poziotinib (3 out of 23),32 and acquired secondary EGFR T790M or C797S mutations have been reported to confer resistance to mobocertinib (1 each out of 9). 12 Although the exact reasons for such difference between sunvozertinib and these EGFR TKIs are currently unknown, one possible mechanism is likely due to their different mechanisms of action.¹³ Preclinically, we also found that sunvozertinib-resistant cells harbored EGFR C797S (Table S7), which was consistent with the clinical findings. EGFR C797S was a known on-target resistance mechanism to the approved third-generation EGFR TKIs for treating patients with EGFRm NSCLC, 33 and similar to EGFR T790M, EGFR C797S was also in cis with exon20ins. Interestingly, for patients with aberrations of both EGFR C797S and exon20ins, the ctDNA mutation abundance of C797S was lower than that of exon20ins, possibly due to intratumor heterogeneity as a consequence of tumor evolution and different speed of clonal evolution. In this analysis, we observed that three patients had detectable EGFR exon20ins at baseline



while EGFR exon20ins was negative in one patient when disease progressed, which may be because of lower shedding level at disease progression compared to that of baseline. In addition, we also observed evolving genetic aberrations of EGFR downstream signaling pathways, e.g., KRAS and PIK3CA mutations, and BRAF amplifications, which also indicate intratumor heterogeneity in resistance. This implied that a combination strategy with inhibition of bypass pathways could be a potentially effective approach for overcoming the resistance. For JAK2 mutation in lung cancer, it was reported that it was detected in plasma samples, but not tumor tissue samples, which may mean somatic mutations detected in the blood samples were from hematopoietic cells' somatic mutations but not from tumors. 34,35 In a publication exploring the mechanisms of resistance to osimertinib in first-line treatment, JAK2 mutation was detected in postdose plasma in the absence of any detectable EGFRm. 36 In our study, JAK2 mutation was detected in the plasma at disease progression with detectable EGFR exon20ins. Further studies may be needed to confirm whether JAK2 mutation was a resistance mechanism of EGFR TKI using paired tumor tissue samples and plasma samples collected at disease progression.

To develop a treatment strategy for overcoming resistance, we generated cell lines that co-expressed EGFR exon20ins and C797S. In the cell lines, we observed that the activity of sunvozertinib was reduced compared with the cell line only expressing EGFR exon20ins mutant protein. These data confirmed that EGFR C797S co-mutations indeed lead to sunvozertinib resistance. In our test, as quite a few common EGFR TKIs have already been reported to be inactive to SVD-C797S, including erlotinib, afatinib, osimertinib, poziotinib, mobocertinib, zipalertinib, furmonertinib, and brigatinib, 37,38 we then tested different approaches to explore potential treatment options. We tested a fourth-generation EGFR TKI that targeted EGFR C797S¹⁵ and found that it could not inhibit cell growth, probably due to lack of activity against EGFR exon20ins. Interestingly, we found that chemotherapy alone or in combination with a JAK inhibitor golidocitinib showed antitumor activity in a sunvozertinib-resistant xenograft model, and the combination showed better effect. This suggested that JAK/STAT pathway blockade in combination with chemotherapy could be a therapeutic approach, which warrants further clinical development.

Taken together, this genetic biomarker analysis of sunvozertinib clinical studies suggests that understanding the genetic biomarkers may have important therapeutic implications for NSCLC with *EGFR* exon20ins, indicating prognosis, providing information to help monitor and identify emerging resistance mechanisms, and guiding treatment.

Limitations of the study

There are some limitations of this study. First, this analysis was based on early-phase clinical trials, which warrant further evaluation. Second, the sample size for exploring drug resistance mechanisms was small. More efforts, such as increasing sample size and obtaining sufficient tumor samples, are needed to discover the full spectrum of sunvozertinib resistance mechanisms.

RESOURCE AVAILABILITY

Lead contact

Further information and requests for resources and reagents should be directed to and will be fulfilled by the lead contact, Mengzhao Wang (mengzhaowang@sina.com).

Materials availability

This study did not generate new unique reagents.

Data and code availability

- The refined mutation data are shown in Tables S1, S2, S4, and S6.
- This paper does not report original code.
- Any additional information required to reanalyze the data reported in this
 paper is available from the lead contact upon request.

ACKNOWLEDGMENTS

These studies were funded by Dizal Pharmaceutical. The authors would like to thank the patients and their families, all investigators, and all investigational site members involved in these studies. The authors are grateful to the investigators shown in Table S8 for their contributions in the independent validation cohort. The authors would also like to thank Dizal Pharmaceutical for the support of statistical analysis and medical writing.

AUTHOR CONTRIBUTIONS

Y.X. and J.C.-H.Y. contributed to conceptualization, data curation, formal analysis, investigation, methodology, project administration, resources, visualization, writing – original draft, and writing – review and editing. Y.Z., L.D., J.Z., Y.W., D.P., Y.F., B.J., Z.H., L.G., J.M., M.S., Y. Hu, X.S., C.D., L.W., K. T., L.L., Y. Yao, Y.C., Y. He, B.P.F., F.G., E.F., J.B.-B., A.L., Y. Yu, X.D., J. G., D.R.C., W.N., C.Z., R.Y., T.J., B.G., L.B., M.N., J.W., X.R., F.X., W.L., D. Z., H.W., S.S., and J.H. contributed to data curation, investigation, resources, and writing – review and editing. X.Z. contributed to data curation, formal analysis, methodology, validation, visualization, writing – review and editing. L.Z. contributed to conceptualization, methodology, project administration, visualization, and writing – review and editing. P.A.J. contributed to conceptualization, data curation, investigation, methodology, resources, supervision, writing – original draft, and writing – review and editing.

DECLARATION OF INTERESTS

Y.X. has received partial research funding from AstraZeneca outside the submitted work. J.C.-H.Y. reports institutional fees from Amgen for advisory works; grants, personal fees, and institutional fee from AstraZeneca for advisory works; institutional fee from Bayer for advisory works; institutional fees from Boehringer Ingelheim for advisory works; institutional fees from Bristol Myers Squibb for advisory works; institutional fee from Daiichi Sankyo for advisory works; institutional fee from Eli Lilly for advisory works; institutional fee from Merck KGaA, Darmstadt, Germany, for advisory works; institutional fee from Merck Sharp & Dohme for advisory works; institutional fee from Novartis for advisory works; institutional fee from Pfizer for advisory works; grants and institutional fee from Roche/Genentech for advisory works; institutional fee and travel fee from Takeda Oncology for advisory works; institutional fee from Yuhan Pharmaceuticals for advisory works; institutional fee from Janssen Pharmaceuticals for advisory works; institutional fee from Gilead Sciences Inc., for advisory works: institutional fee from GSK for advisory works: personal fee from BeiGene for advisory works; institutional fee from Regeneron Pharmaceutical for advisory works; institutional fee from ArriVent for advisory works; institutional fee from AnHeart Therapeutics for advisory works; and travel fee from Dizal Pharmaceuticals to major conference. D.P. reports consulting, advisory role, or lectures: AstraZeneca, AbbVie, Bristol Myers Squibb, Boehringer Ingelheim, Celgene, Daiichi Sankyo, Eli Lilly, Merck, Novartis, Janssen, Pfizer, Roche, Pierre Fabre, Takeda, ArriVent, Mirati, Seagen,

Article



and GSK; clinical trial research as a principal investigator or co-investigator (institutional financial interests): AstraZeneca, Bristol Myers Squibb, Boehringer Ingelheim, Eli Lilly, Merck, Novartis, Pfizer, Roche, Medimmune, Sanofi-Aventis, Taiho Pharma, Novocure, Daiichi Sankyo, AbbVie, Janssen, Pierre Fabre, Takeda, ArriVent, Mirati, and Seagen; and travel, accommodations, and expenses: AstraZeneca, Roche, Novartis, and Pfizer. B.P.F. receives research support from Bristol Myers Squibb Foundation, Guardant Health, Bayer, Merck/MSD, Foundation Medicine, Illumina, Regeneron, AstraZeneca, Merus, Gilead, Catalyst, and OncoHost. E.F. reports receipt of personal honoraria for advisory board participation from AbbVie, Amgen, AstraZeneca, Bayer, Boehringer Ingelheim, BMS, Daiichi Sankyo, F. Hoffmann-La Roche, Genmab, Gilead, GSK, ITeos Therapeutics, Janssen, Johnson & Johnson, MSD, Novartis, Pierre Fabre, Pfizer, Regeneron, Turning Point, and Daiichi Sankyo; personal speaker honoraria from Amgen, AstraZeneca, BMS, Daiichi Sankyo, Eli Lilly, F. Hoffmann-La Roche, Johnson & Johnson, Genentech, Gilead, Janssen, Medical Trends, Medscape, Merck Serono, MSD, Novartis, PeerVoice, Pierre Fabre, Pfizer, Regeneron, and Touch Oncology; Board of Director role: Grifols; and financial support for meeting attendance and/or travel from AstraZeneca, Janssen, and Roche. E.F. is a principal investigator in trials (institutional financial support for clinical trials) sponsored by AstraZeneca, AbbVie, Amgen, Bayer, BeiGene, Boehringer Ingelheim, BMS, Daiichi Sankyo, Exelixis, F. Hoffmann-La Roche, Genentech, GSK, Janssen, MSD, Merck KGAA, Mirati, Novartis, Nuvalent, Pfizer, and Takeda. J.B.-B. reports personal fees from advisory boards (MSD and Roche); educational lectures from BMS, AstraZeneca, Pfizer, Takeda, Regeneron, Amgen, Merck, and Sanofi, outside the submitted work; and has received support for attending meetings and/or travel from Takeda, MSD, and Roche. D.R.C.: Ad hoc consulting Dizal. L.B. has received consulting fees from Pfizer, An-Heart, AstraZeneca, Regeneron, Genentech, Janssen, Novocure, Bayer, Daichi, BMS, Sanofi, Gilead, Teligene, BI, BioAtla, and Neuvogen. M.N. is on the advisory board for AstraZeneca, Daiichi Sankyo, Takeda, Novartis, EMD Serono, Janssen, Pfizer, Eli Lilly and Company, Bayer, Regeneron, BMS, and Genentech; a consultant for Caris Life Sciences (virtual tumor board); a speaker for Blueprint Medicines, Janssen, Mirati, and Takeda; reports travel support from AnHeart Therapeutics; and reports stock/stock options from MBrace Therapeutics. X.Z. and L.Z. are employees of Dizal Pharmaceutical and hold stock in Dizal Pharmaceutical. P.A.J.'s institution has received research funding from AstraZeneca, Daiichi Sankyo, PUMA, Eli Lilly, Boehringer Ingelheim, Revolution Medicines, and Takeda Oncology. P.A.J. reports consulting fees from AstraZeneca, Boehringer Ingelheim, Pfizer, Roche/ Genentech, Chugai Pharmaceuticals, Eli Lilly pharmaceuticals, SFJ Pharmaceuticals, Voronoi, Daiichi Sankyo, Biocartis, Novartis, Takeda Oncology, Mirati Therapeutics, Transcenta, Silicon Therapeutics, Syndax, Nuvalent, Bayer, Esai, Allorion Therapeutics, Accutar Biotech, AbbVie, Monte Rosa, Scorpion Therapeutics, Merus, Frontier Medicines, Hongyun Biotechnology, Duality, Blueprint Medicines, and Dizal Pharmaceuticals; stock in Gatekeeper Pharmaceuticals; and a patent for EGFR mutations issued, licensed, and with royalties paid by LabCorp.

STAR*METHODS

Detailed methods are provided in the online version of this paper and include the following:

- KEY RESOURCES TABLE
- EXPERIMENTAL MODEL AND STUDY PARTICIPANT DETAILS
 - Human subjects
 - Cell culture and cell lines
 - Animal experiments
- METHOD DETAILS
 - o Study design and endpoints
 - o Plasma sampling and ctDNA extraction
 - o NGS of plasma ctDNA
 - o Droplet digital PCR of plasma ctDNA
 - $\circ \ \, \text{Cell proliferation assay}$
 - Western blotting
 - Immunohistochemical (IHC) staining and analysis

- QUANTIFICATION AND STATISTICAL ANALYSIS
- ADDITIONAL RESOURCES

SUPPLEMENTAL INFORMATION

Supplemental information can be found online at https://doi.org/10.1016/j.xcrm.2025.102121.

Received: October 9, 2024 Revised: February 1, 2025 Accepted: April 10, 2025 Published: May 6, 2025

REFERENCES

- Arcila, M.E., Nafa, K., Chaft, J.E., Rekhtman, N., Lau, C., Reva, B.A., Zakowski, M.F., Kris, M.G., and Ladanyi, M. (2013). EGFR exon 20 insertion mutations in lung adenocarcinomas: prevalence, molecular heterogeneity, and clinicopathologic characteristics. Mol. Cancer Ther. 12, 220–229.
- Bauml, J.M., Viteri, S., Minchom, A., Bazhenova, L., Ou, S., Schaffer, M., Le Croy, N., Riley, R., Mahadevia, P., and Girard, N. (2021). FP07.12 underdiagnosis of EGFR exon 20 insertion mutation variants: estimates from NGS-based real-world datasets. J. Thorac. Oncol. 16, S208–S209
- 3. Kim, B.G., Jang, J.H., Kim, J.W., Shin, S.H., Jeong, B.H., Lee, K., Kim, H., Kwon, O.J., Ahn, M.J., and Um, S.W. (2022). Clinical Utility of Plasma Cell-Free DNA EGFR Mutation Analysis in Treatment-Naïve Stage IV Non-Small Cell Lung Cancer Patients. J. Clin. Med. 11, 1144.
- Karachaliou, N., Mayo-de-Las-Casas, C., Molina-Vila, M.A., and Rosell, R. (2015). Real-time liquid biopsies become a reality in cancer treatment. Ann. Transl. Med. 3, 36.
- Alix-Panabières, C., and Pantel, K. (2016). Clinical Applications of Circulating Tumor Cells and Circulating Tumor DNA as Liquid Biopsy. Cancer Discour. 6, 479, 491.
- Kilgour, E., Rothwell, D.G., Brady, G., and Dive, C. (2020). Liquid Biopsy-Based Biomarkers of Treatment Response and Resistance. Cancer Cell 27, 485, 405.
- Wang, M., Fan, Y., Sun, M., Wang, Y., Zhao, Y., Jin, B., Hu, Y., Han, Z., Song, X., Liu, A., et al. (2024). Sunvozertinib for patients in China with platinum-pretreated locally advanced or metastatic non-small-cell lung cancer and EGFR exon 20 insertion mutation (WU-KONG6): singlearm, open-label, multicentre, phase 2 trial. Lancet Respir. Med. 12, 217, 224
- Wu, S.G., and Shih, J.Y. (2018). Management of acquired resistance to EGFR TKI-targeted therapy in advanced non-small cell lung cancer. Mol. Cancer 17, 38.
- Jackman, D., Pao, W., Riely, G.J., Engelman, J.A., Kris, M.G., Jänne, P. A., Lynch, T., Johnson, B.E., and Miller, V.A. (2010). Clinical definition of acquired resistance to epidermal growth factor receptor tyrosine kinase inhibitors in non-small-cell lung cancer. J. Clin. Oncol. 28, 357-360
- Thress, K.S., Paweletz, C.P., Felip, E., Cho, B.C., Stetson, D., Dougherty, B., Lai, Z., Markovets, A., Vivancos, A., Kuang, Y., et al. (2015). Acquired EGFR C797S mutation mediates resistance to AZD9291 in non-small cell lung cancer harboring EGFR T790M. Nat. Med. 21, 560–562.
- Niederst, M.J., Hu, H., Mulvey, H.E., Lockerman, E.L., Garcia, A.R., Piotrowska, Z., Sequist, L.V., and Engelman, J.A. (2015). The Allelic Context of the C797S Mutation Acquired upon Treatment with Third-Generation EGFR Inhibitors Impacts Sensitivity to Subsequent Treatment Strategies. Clin. Cancer Res. 21, 3924–3933.
- 12. Park, S., Park, S., Kim, T.M., Kim, S., Koh, J., Lim, J., Yi, K., Yi, B., Ju, Y.S., Kim, M., et al. (2024). Resistance mechanisms of EGFR tyrosine kinase



- inhibitors, in EGFR exon 20 insertion-mutant lung cancer. Eur. J. Cancer 208. 114206.
- Wang, M., Yang, J.C.H., Mitchell, P.L., Fang, J., Camidge, D.R., Nian, W., Chiu, C.H., Zhou, J., Zhao, Y., Su, W.C., et al. (2022). Sunvozertinib, a Selective EGFR Inhibitor for Previously Treated Non-Small Cell Lung Cancer with EGbib31FR Exon 20 Insertion Mutations. Cancer Discov. 12, 1676–1689
- 14. Yang, J.C., Doucet, L., Wang, M., Fan, Y., Sun, M., Greillier, L., Planchard, D., Mazieres, J., Felip, E., Pellini, B., et al. (2024). A multinational pivotal study of sunvozertinib in platinum pretreated non-small cell lung cancer with EGFR exon 20 insertion mutations: Primary analysis of WU-KONG1 study [Abstract]. J. Clin. Oncol. 42, Number_16_suppl.
- 15. Lucas, M.C., Merchant, M.S., O'Connor, M., Cook, C., Smith, S., Trombino, A., Zhang, W.Y., Visiers, I., Tith, K., and Foroughi, R. (2021). BDTX-1535, a CNS penetrant MasterKey inhibitor of common, uncommon and resistant EGFR mutations, demonstrates in vivo efficacy and has potential to treat osimertinib-resistant NSCLC with or without brain metastases [abstract]. Mol. Cancer Ther. 20, P02–P04.
- Kim, S.M., Kwon, O.J., Hong, Y.K., Kim, J.H., Solca, F., Ha, S.J., Soo, R.A., Christensen, J.G., Lee, J.H., and Cho, B.C. (2012). Activation of IL-6R/ JAK1/STAT3 signaling induces de novo resistance to irreversible EGFR inhibitors in non-small cell lung cancer with T790M resistance mutation. Mol. Cancer Ther. 11, 2254–2264.
- de Haas, N., de Koning, C., Spilgies, L., de Vries, I.J.M., and Hato, S.V. (2016). Improving cancer immunotherapy by targeting the STATe of MDSCs. Oncolmmunology 5, e1196312.
- Song, Y., Yoon, D.H., Yang, H., Cao, J., Ji, D., Koh, Y., Jing, H., Eom, H., Kwak, J., Lee, W., et al. (2023). Phase I dose escalation and expansion study of golidocitinib, a highly selective JAK1 inhibitor, in relapsed or refractory peripheral T-cell lymphomas. Ann. Oncol. 34, 1055–1063.
- Li, W., Liu, J.B., Hou, L.K., Yu, F., Zhang, J., Wu, W., Tang, X.M., Sun, F., Lu, H.M., Deng, J., et al. (2022). Liquid biopsy in lung cancer: significance in diagnostics, prediction, and treatment monitoring. Mol. Cancer 21, 25.
- Zhou, C., Tang, K.J., Cho, B.C., Liu, B., Paz-Ares, L., Cheng, S., Kitazono, S., Thiagarajan, M., Goldman, J.W., Sabari, J.K., et al. (2023). Amivantamab plus Chemotherapy in NSCLC with EGFR Exon 20 Insertions. N. Engl. J. Med. 389, 2039–2051.
- Zhou, C., Ramalingam, S.S., Kim, T.M., Kim, S.W., Yang, J.C.H., Riely, G. J., Mekhail, T., Nguyen, D., Garcia Campelo, M.R., Felip, E., et al. (2021). Treatment Outcomes and Safety of Mobocertinib in Platinum-Pretreated Patients With EGFR Exon 20 Insertion-Positive Metastatic Non-Small Cell Lung Cancer: A Phase 1/2 Open-label Nonrandomized Clinical Trial. JAMA Oncol. 7, e214761.
- Jänne, P.A., Wang, B.C., Cho, B.C., Zhao, J., Li, J., Hochmair, M., Peters, S., Besse, B., Pavlakis, N., Neal, J.W., et al. (2025). First-Line Mobocertinib Versus Platinum-Based Chemotherapy in Patients With EGFR Exon 20 Insertion-Positive Metastatic Non-Small Cell Lung Cancer in the Phase III EXCLAIM-2 Trial. J. Clin. Oncol. 29, JCO2401269.
- Normanno, N., Denis, M.G., Thress, K.S., Ratcliffe, M., and Reck, M. (2017). Guide to detecting epidermal growth factor receptor (EGFR) mutations in ctDNA of patients with advanced non-small-cell lung cancer. Oncotarget 8, 12501–12516.
- 24. Neal, J.W., Li, Y., Yu, Z., Fram, R.J., Danes, C., Vincent, S., and Piotrowska, Z. (2023). Mobocertinib efficacy in patients with NSCLC and EGFR exon 20 insertion mutations (ex20ins) identified by next-generation sequencing (NGS) of circulating tumor DNA (ctDNA) [Abstract]. J. Clin. Oncol. 41, 9082. Number 16_suppl.
- Mack, P.C., Miao, J., Redman, M.W., Moon, J., Goldberg, S.B., Herbst, R. S., Melnick, M.A., Walther, Z., Hirsch, F.R., Politi, K., et al. (2022). Circulating Tumor DNA Kinetics Predict Progression-Free and Overall Survival in EGFR TKI-Treated Patients with EGFR-Mutant NSCLC (SWOG S1403). Clin. Cancer Res. 28, 3752–3760.

- Adashek, J.J., Janku, F., and Kurzrock, R. (2021). Signed in Blood: Circulating Tumor DNA in Cancer Diagnosis, Treatment and Screening. Cancers 13, 3600.
- 27. Gray, J.E., Ahn, M.J., Oxnard, G.R., Shepherd, F.A., Imamura, F., Cheng, Y., Okamoto, I., Cho, B.C., Lin, M.C., Wu, Y.L., et al. (2023). Early Clearance of Plasma Epidermal Growth Factor Receptor Mutations as a Predictor of Outcome on Osimertinib in Advanced Non-Small Cell Lung Cancer; Exploratory Analysis from AURA3 and FLAURA. Clin. Cancer Res. 29, 3340–3351.
- 28. Jänne, P.A., Kobayashi, K., Robichaux, J., Lee, C.K., Sugawara, S., Yang, T.Y., Kim, T.M., Yanagitani, N., Kim, S.W., Markovets, A., et al. (2024). FLAURA2: exploratory analysis of baseline (BL) and on-treatment plasma EGFRm dynamics in patients (pts) with EGFRm advanced NSCLC treated with first-line (1L) osimertinib (osi) ± platinum-pemetrexed [abstract]. In Proceedings of the American Association for Cancer Research Annual Meeting 2024; Part 2 (Late-Breaking, Clinical Trial, and Invited Abstracts); 2024 Apr 5-10; San Diego, CA. Philadelphia (PA): AACR; Cancer Res., 84, p. CT017.
- Vincent, S., Su, Z., Bunn, V., Joshi, A., Yu, Z., Chatterjee, S., Guha, M., and Zhang, P. (2022). Molecular analysis of circulating tumor DNA (ctDNA) in patients (pts) with EGFR exon 20 insertion-positive (ex20ins+) advanced NSCLC treated with mobocertinib [Abstract]. J. Clin. Oncol. 40, Number_16_suppl.
- Ma, S., Shi, M., Chen, X., Wang, Y., Yang, Z., Lizaso, A., Li, M., Li, H., Zhang, L., Mao, X., et al. (2021). The prognostic value of longitudinal circulating tumor DNA profiling during osimertinib treatment. Transl. Lung Cancer Res. 10, 326–339.
- Yamaguchi, O., Kasahara, N., Soda, H., Imai, H., Naruse, I., Yamaguchi, H., Itai, M., Taguchi, K., Uchida, M., Sunaga, N., et al. (2023). Predictive significance of circulating tumor DNA against patients with T790M-positive EGFR-mutant NSCLC receiving osimertinib. Sci. Rep. 13, 20848.
- Elamin, Y.Y., Robichaux, J.P., Carter, B.W., Altan, M., Tran, H., Gibbons, D.L., Heeke, S., Fossella, F.V., Lam, V.K., Le, X., et al. (2022). Poziotinib for EGFR exon 20-mutant NSCLC: Clinical efficacy, resistance mechanisms, and impact of insertion location on drug sensitivity. Cancer Cell 40, 754– 767 e6.
- He, J., Huang, Z., Han, L., Gong, Y., and Xie, C. (2021). Mechanisms and management of 3rd-generation EGFR-TKI resistance in advanced nonsmall cell lung cancer (Review). Int. J. Oncol. 59, 90.
- 34. Le, X., Puri, S., Negrao, M.V., Nilsson, M.B., Robichaux, J., Boyle, T., Hicks, J.K., Lovinger, K.L., Roarty, E., Rinsurongkawong, W., et al. (2018). Landscape of EGFR-Dependent and -Independent Resistance Mechanisms to Osimertinib and Continuation Therapy Beyond Progression in EGFR-Mutant NSCLC. Clin. Cancer Res. 24, 6195–6203.
- 35. Xu, Y., Jin, J., Xu, J., Shao, Y.W., and Fan, Y. (2017). JAK2 variations and functions in lung adenocarcinoma. Tumour Biol. 39, 1010428317711140.
- Ramalingam, S.S., Yang, J.C.H., Lee, C.K., Kurata, T., Kim, D.W., John, T., Nogami, N., Ohe, Y., Mann, H., Rukazenkov, Y., et al. (2018). Osimertinib As First-Line Treatment of EGFR Mutation-Positive Advanced Non-Small-Cell Lung Cancer. J. Clin. Oncol. 36, 841–849.
- 37. Hamada, A., Suda, K., Nishino, M., Obata, K., Oiki, H., Fukami, T., Fukuda, S., Fujino, T., Ohara, S., Koga, T., et al. (2024). Secondary Mutations of the EGFR Gene That Confer Resistance to Mobocertinib in EGFR Exon 20 Insertion. J. Thorac. Oncol. 19, 71–79.
- Kobayashi, I.S., Shaffer, W., Viray, H., Rangachari, D., VanderLaan, P.A., Kobayashi, S.S., and Costa, D.B. (2023). The Impact of On-Target Resistance Mediated by EGFR-T790M or EGFR-C797S on EGFR Exon 20 Insertion Mutation Active Tyrosine Kinase Inhibitors. JTO Clin. Res. Rep. 5, 100614
- Eisenhauer, E.A., Therasse, P., Bogaerts, J., Schwartz, L.H., Sargent, D., Ford, R., Dancey, J., Arbuck, S., Gwyther, S., Mooney, M., et al. (2009). New response evaluation criteria in solid tumours: revised RECIST guide-line (version 1.1). Eur. J. Cancer 45, 228–247.

Article



- Mao, X., Zhang, Z., Zheng, X., Xie, F., Duan, F., Jiang, L., Chuai, S., Han-Zhang, H., Han, B., and Sun, J. (2017). Capture-based targeted ultradeep sequencing in paired tissue and plasma samples demonstrates differential subclonal ctDNA-releasing capability in advanced lung cancer. J. Thorac. Oncol. 12, 663–672.
- 41. Li, Y.S., Jiang, B.Y., Yang, J.J., Zhang, X.C., Zhang, Z., Ye, J.Y., Zhong, W. Z., Tu, H.Y., Chen, H.J., Wang, Z., et al. (2018). Unique genetic profiles
- from cerebrospinal fluid cell-free DNA in leptomeningeal metastases of EGFR-mutant non-small-cell lung cancer: a new medium of liquid biopsy. Ann. Oncol. 29, 945–952.
- 42. Zhu, G., Ye, X., Dong, Z., Lu, Y.C., Sun, Y., Liu, Y., McCormack, R., Gu, Y., and Liu, X. (2015). Highly Sensitive Droplet Digital PCR Method for Detection of EGFR-Activating Mutations in Plasma Cell-Free DNA from Patients with Advanced Non-Small Cell Lung Cancer. J. Mol. Diagn. 17, 265–272.



STAR*METHODS

KEY RESOURCES TABLE

REAGENT or RESOURCE	SOURCE	IDENTIFIER
Antibodies		
pEGFR (Tyr1068)	Cell Signaling Technology	Cat# 2234; RRID: AB_331701
EGFR	Cell Signaling Technology	Cat# 4267; RRID: AB_2246311
GAPDH	Cell Signaling Technology	Cat# 2118; RRID: AB_561053
pSTAT3(Tyr705)	Cell Signaling Technology	Cat# 9145; RRID: AB_2491009
Biological samples		
Human plasma	This paper	N/A
Kenograft tumor tissue	Xenograft model in this study	N/A
Chemicals, peptides, and recombinant proteins		
BDTX-1535	Haoyuan Biotechnology Co Ltd	N/A
Sunvozertinib	Dizal Pharmaceutical	N/A
Critical commercial assays		<u> </u>
QIAamp Circulating Nucleic Acid Kit	Qiagen	Cat# 55114
OncoCompass [™] Target Cancer Mutation Profiling Liquid Kit	Burning Rock Biotech	N/A
ddPCR TM Supermix for Probes (No dUTP)	Bio-Rad	Cat# 1863024
BstUI	NEB	Cat# R0518L
Automated Droplet Generation Oil for Probes	Bio-Rad	Cat# 186-4110
Deposited data		
nformed mutation data	This paper	Tables S1, S2, S4, and S6
Experimental models: Cell lines		
Ba/F3 EGFR SVD-C797S	KYINNO biotechnology	Cat# KC-2509
Ba/F3	Riken	RCB0805
KLN205	ATCC	CRL-1453
Experimental models: Organisms/strains		
DBA/2 mice	Beijing Vital River Laboratory Animal Technology Co., Ltd	N/A
Oligonucleotides		
Primers used for ddPCR	This paper	Tables S9 and S10
Probes used for ddPCR	This paper	Tables S11 and S12
String DNA used for ddPCR	This paper	Tables S13 and S14
Software and algorithms		
GraphPad Prism v10	GraphPad Software	www.graphpad.com
QuantaSoft software	Bio-Rad	www.bio-rad.com
magescope software version 12.4.6	Leica Biosystems	www.leicabiosystems.com
SAS software version 9.4	SAS Institute	www.sas.com
XLFit software version 5.5.0	IDBS	www.idbs.com/xlfit

EXPERIMENTAL MODEL AND STUDY PARTICIPANT DETAILS

Human subjects

The biomarker analysis presented here were based on analysis of plasma ctDNA specimens obtained from 121 patients who participated in WU-KONG1A (24 patients), WU-KONG2 dose expansion (18 patients) and WU-KONG6 (79 patients) clinical studies (Figure S12). Full details of the WU-KONG1, WU-KONG2 and WU-KONG6 studies have been previously described.^{7,13} In these studies, patients with locally advanced or metastatic NSCLC with *EGFR* exon20ins were enrolled and treated with sunvozertinib at doses from 50 to 400 mg QD, in 21-day cycles to evaluate the efficacy of sunvozertinib. In these studies, the efficacy endpoints included ORR and PFS, assessed by investigators per Response Evaluation Criteria In Solid Tumors (RECIST), version 1.1.³⁹

Article



Sixty-three patients included in the independent validation cohort were from a phase 2, multinational pivotal clinical study WU-KONG1B (Figure S13). WU-KONG1B is a study to assess the antitumor efficacy of sunvozertinib at two dose levels, 200 mg and 300 mg, in platinum pre-treated patients with *EGFR* exon20ins NSCLC. Eligible patients were randomized at the ratio of 1:1 to receive 200 mg or 300 mg sunvozertinib once daily until discontinuation criteria were met. The primary endpoint was blinded Independent Review Committee (IRC) assessed ORR according to RECIST v1.1.¹⁴

The studies received institutional review board or ethics committee approval at all participating centers, and all patients provided informed consent prior to entry into the studies. The studies were undertaken in accordance with the Declaration of Helsinki and Good Clinical Practice guidelines, as defined by the International Council on Harmonization.

Cell culture and cell lines

The interleukin (IL)-3-dependent Ba/F3 cell line and murine lung cancer cell line KLN205 were obtained from Riken and ATCC, respectively. Ba/F3 cell line harboring *EGFR* V769_D770insASV (ASV), D770_N771insSVD (SVD), H773_V774insNPH (NPH) were established in our previous study. Ba/F3 cells carrying *EGFR* SVD-C797S was purchased from KYINNO biotechnology (Cat.# KC-2509, Beijing, China). KLN205 cell line carrying *EGFR* SVD-C797S was generated as below:

Full-length cDNAs of human *EGFR* (NM005228.3) containing SVD-C797S were generated at Shanghai Sunbio Biotechnology Co., Ltd (Shanghai, China) and confirmed by Sanger sequencing. The cDNAs were then subcloned into pMT143 lentiviral vector (Shanghai Sunbio Biotechnology Co., Ltd). The lentivirus was packaged in 293T/17 cells (ATCC Cat# CRL-11268, RRID: CVCL_1926) by transfection of lentiviral constructs and packaging mix (Shanghai Sunbio Biotechnology Co., Ltd). Then KLN205 cells were infected by lentivirus with 5 μ g/ml polybrene (Sigma-Aldrich, St. Louis, MO, USA), selected in 2 μ g/mL puromycin (Invitrogen, Carlsbad, CA, USA) as single cell clones, and maintained in 1 μ g/mL puromycin with IL-3 depletion. Expression of exogenous EGFR variants in Ba/F3 cells and KLN205 cells were confirmed by Sanger sequencing at mRNA level.

The obtained single cell clones were cultured in RPMI1640 medium with 10% fetal bovine serum and 1 μ g/mL puromycin and maintained in a humidified incubator at 37°C with 5% CO₂.

BaF3 cells have been authenticated by short tandem repeat profiling and cross-species check. KLN205 cells have been authenticated by cross-species check. All cell lines were routinely checked for mycroplasma contamination free.

To investigate the potential acquired resistance mutations of sunvozertinib, Ba/F3 cells harboring the most common *EGFR* exon20ins (SVD, ASV, or NPH) were chronically exposed to escalating concentrations of sunvozertinib until resistance clones developed. These clones were then subjected to test by ddPCR.

Animal experiments

All studies involving animals were conducted according to the guidelines approved by Institutional Animal Care and Use Committees (IACUC). Six- to eight-week-old specific-pathogen-free immunocompromised female DAB/2 mice were purchased from Beijing Vital River Laboratory Animal Technology Co., Ltd.

KLN205 cell clones expressing EGFR SVD-C797S were injected subcutaneously into the dorsal flank of female immune-compromised DBA/2 mice. Tumor nodules were measured in two dimensions with caliper and the tumor volume was calculated using the following formula: tumor volume = (length x width²) x 0.52. When the mean tumor volume reached 150 to 250 mm³, tumor-bearing mice were randomized into different treatment groups. Mice were then treated from the day post randomization. Mice in vehicle control received 0.5% HPMC/0.1% Tween 80 orally (p.o) twice daily (bid). Sunvozertinib was given orally at 25 mg/kg bid, while pemetrexed was administered intraperitoneally (i.p) at 100 mg/kg twice weekly (biw), cisplatin was administered i.p at 4 mg/kg biw. The combination groups received pemetrexed or cisplatin with sunvozertinib concurrently. The tumor volume and body weight of the mice were measured twice weekly. Tumor growth inhibition from start of treatment was assessed by comparison of the mean change in tumor volume between the control and treatment groups and presented as tumor growth inhibition. The arithmetic mean tumor volume was used for efficacy calculation. The calculation was based on the arithmetic mean of relative tumor volume (RTV) in each group. RTV was calculated by dividing the tumor volume on the treatment day with the initial tumor volume. The efficacy of tumor growth inhibition on specific day, for each treated group, was calculated by formula: Inhibition % = (CG-TG) x 100 / (CG-1), among which "CG" means the arithmetic mean of RTV of the treated group.

METHOD DETAILS

Study design and endpoints

The biomarker analysis presented here were exploratory, which was conducted retrospectively using plasma ctDNA specimens. In WU-KONG1A, WU-KONG1B, WU-KONG2 dose expansion and WU-KONG6 cohorts, patients with locally advanced or metastatic NSCLC with EGFR exon20ins, who had received at least one prior line of system anti-cancer therapy, treated with sunvozertinib at the doses \geq 200 mg QD, were included in this biomarker analysis.

Plasma sampling and ctDNA extraction

In WU-KONG1A, WU-KONG1B and WU-KONG6 studies, serial plasma specimens from baseline (before the first dose of sunvozer-tinib) until disease progression, including baseline, Cycle 1 Day 8, Cycle 1 Day 15, Cycle 2 Day 1, then every 3 weeks until



Cycle 6 Day 1, and every 6 weeks afterwards until disease progression, were collected (Figure S14). In WU-KONG2 dose expansion cohort, plasma specimens at baseline and disease progression were collected. Plasma ctDNA samples at baseline were analyzed by NGS to explore *EGFR* exon20ins status and abundance. In addition, plasma ctDNA samples collected at baseline and timepoint around disease progression were analyzed by NGS to explore the potential resistance mechanisms of sunvozertinib on subjects meeting the criteria for acquired resistance to sunvozertinib. Serial plasma specimens collected from baseline until disease progression were analyzed by ddPCR to dynamically monitor *EGFR* exon20ins quantity. QIAamp Circulating Nucleic Acid Kit (Qiagen, Hilden, Germany) was used for ctDNA extraction from plasma samples following the manufacturer's protocol.

NGS of plasma ctDNA

NGS analysis of plasma ctDNA samples was conducted using capture-based OncoCompassTM Target Cancer Mutation Profiling Liquid Kit (Burning Rock Biotech, Guangzhou, China) following optimized protocols as described previously. ^{40,41} Genetic alterations in *EGFR* and genes in EGFR downstream signaling pathways were analyzed, including *AKT1*, *BRAF*, *CTNNB1*, *EGFR*, *ERBB2*, *HRAS*, *JAK1*, *JAK2*, *KIT*, *KRAS*, *MAP2K1*, *MET*, *MTOR*, *MYC*, *NF1*, *NRAS*, *PIK3CA*, *PIK3CG*, *PIK3R1*, *PTEN*, *RAF1* and *TP53*.

Droplet digital PCR of plasma ctDNA

We developed *EGFR* exon20ins and C797S ddPCR assays in a similar fashion as previously described for other *EGFR* mutations. ⁴² In brief, we designed primer and probe pairs (Tables S9–S12) and optimized them for annealing temperature and cycling condition using serial dilutions of mutant DNA (GeneArt Strings DNA Fragments) (Tables S13 and S14). The *EGFR* exon20ins ddPCR assay achieved a theorical ddPCR limit of detection of 0.05% (one mutant in 2000 wild-type molecules). The *EGFR* C797S assay achieved a theorical ddPCR limit of detection of 0.1% (one mutant in 1000 wild-type molecules). Notably, in plasma specimens, the detection of mutant molecules is also affected by the quantity of cell-free DNA in the plasma specimen. We purchased ddPCR reagents from Bio-Rad (Bio-Rad, Hercules, CA, USA), ordered GeneArt Strings DNA Fragments and probes from Thermo Fisher Scientific (Thermo Fisher Scientific, Waltham, MA, USA), and ordered primers from Takara (Takara Biotechnology, Dalian, China). Droplets were generated using the Droplet Generator (Bio-Rad), and analyzed with the QX200 Droplet Reader (Bio-Rad) according to the manufacturer's protocol. The ddPCR data analysis was performed with QuantaSoft analysis software (Bio-Rad).

Cell proliferation assay

Cells expressing EGFR exon20ins were seeded in 384-well plates at 1,250 cells/well in RPMI1640 medium containing 10% FBS. At the same time, a day 0 plate was prepared with duplicate rows of each cell line. After overnight incubation, the assay plates were dosed with sunvozertinib. Alongside dosing the assay plates, the day 0 plate was processed using CellTiter–Glo assay to measure the number of viable cells (G_0). The assay plates were further incubated for 72 hours and the number of viable cells (G_0) was measured by CellTiter–Glo assay. The percentage of proliferation was calculated as: % Proliferation = 100 x (G_0 value of sample well - G_0 value)/ (G_0 value of DMSO control - G_0 value). The concentration of compound producing 50% proliferation inhibition (G_0) was further calculated in best-fit curves using XLFit software (IDBS).

Western blotting

Cells were plated at 300,000 cells/well in 6-well plates and dosed for 4 hours with serial dilution of compound. Crude cell lysate was prepared with SDS buffer (0.06 M Tris-HCl pH 6.8, 1% SDS, 10% glycerol) and protein concentration was determined using the Pierce BCA Protein Assay. Total protein (30 µg) was loaded onto SDS PAGE for Western blotting. pEGFR (Tyr1068) antibody (CST#2234), EGFR antibody (CST#4267), and GAPDH antibody (CST#2118) were purchased from Cell Signaling Technology (Boston, USA).

Immunohistochemical (IHC) staining and analysis

Xenograft tissues were obtained from the KLN205 *EGFR* SVD-C797S xenograft model at the last day of treatment. Samples were harvested following by formalin fixation and paraffin embedding (FFPE) for analysis. IHC was performed on 3 μm FFPE sections by using a Ventana automation (Roche) pSTAT3 IHC staining. The historical cases with positive staining of the antibodies were used as positive controls. Tris-buffered saline with Tween 20 was used as negative control. The stained IHC slides were firstly reviewed and interpreted by a qualified pathologist and then quantified by Imagescope software (Leica Biosystems, Buffalo Grove, USA). "H" score was also performed when the cases were illegible on Imagescope software and analyzed statistically by one-way ANOVA with Dunnett test.

QUANTIFICATION AND STATISTICAL ANALYSIS

The data cutoff dates of clinical efficacy data in WU-KONG1A, WU-KONG6, WU-KONG2 and WU-KONG1B studies were September 15, 2023, April 3, 2023, September 27, 2021 and July 29, 2024, respectively. Statistical analyses were performed using SAS software (SAS Institute, NC, USA). Demographic and clinical characteristics and clinical response based on the *EGFR* exon20ins status were compared using the Fisher's Exact Test for categorical variables and the Mann-Whitney test for continuous variables. The Mann-Whitney test was also applied to analyze the correlation between *EGFR* exon20ins abundance and demographic/clinical



characteristics as well as clinical response. Log-rank test was utilized to compare the PFS between different subgroups. Pearson's correlation coefficient was used to measure the correlation between the mutant allele frequency of *EGFR* exon20ins tested by NGS and ddPCR. Significance was established when the *p* value was less than 0.05. All tests were two-sided. The figures presented were created using the GraphPad Prism v10 (GraphPad Software).

For analyzing the data from the *in vitro* and *in vivo* experiments, figures and statistical procedures were performed using GraphPad Prism v10. Two-way ANOVA analysis was used to compare the tumor growth inhibition between groups. One-way ANOVA with Dunnett test was used to compare the pSTAT3 signals and EGFR expression between groups.

ADDITIONAL RESOURCES

WU-KONG1 and WU-KONG6 studies have been registered on "clinicalTrials.gov", the registration IDs are NCT03974022 (https://clinicaltrials.gov/study/NCT03974022) and NCT05712902 (https://clinicaltrials.gov/study/NCT05712902?term=NCT05712902&rank=1), respectively. WU-KONG2 study has been registered on "chinadrugtrial.org.cn", the registration ID is CTR20192097 (http://www.chinadrugtrials.org.cn/clinicaltrials.searchlist.dhtml?reg_no=CTR20192097&indication=&case_no=&drugs_name=&drugs_type=&appliers=&communities=&researchers=&agencies=&state=).